The *Drosophila* synaptotagmin-like protein bitesize is required for growth and has mRNA localization sequences within its open reading frame

Julia Serano* and Gerald M. Rubin

Howard Hughes Medical Institute and Department of Molecular and Cell Biology, University of California, Berkeley, CA 94720-3200

Contributed by Gerald M. Rubin, September 8, 2003

The vertebrate synaptotagmin-like protein granuphilin binds to the vesicle-trafficking proteins Rab27a and Munc18 and can modulate exocytosis of insulin-containing secretory granules in pancreatic beta cell lines. Here, we report the molecular and genetic characterization of bitesize, a granuphilin homolog and the only *Drosophila* synaptotagmin-like protein. Mutations that affect bitesize have reduced cell size and number, resulting in smaller animals that develop slowly. We also show that at least two classes of *bitesize* transcripts are localized to the apical plasma membrane in polarized epithelial cells. Whereas most cis-acting mRNA localization sequences map to 3′ untranslated regions, *bitesize* contains a 2.2-kb sequence within its ORF that is necessary and sufficient for apical localization. Thus, we have found that *bitesize* is a metazoan example of a transcript for which all identifiable mRNA localization sequences are contained within the protein-coding region.

Exocytosis is the process by which intracellular vesicles fuse with the cell membrane, thereby releasing their internal contents into the extracellular environment. For certain neurotransmitters, proteases, peptide hormones, and growth factors, the localization and timing of exocytosis are crucial to ensure the proper execution of cell-signaling events. Many proteins known to regulate various aspects of vesicle trafficking and fusion, such as synaptotagmins (1), rabphilin-3 (2), Rims (3), Doc2 (4), and Unc-13 proteins (5), share a common motif of two C2 domains, which are often located adjacent to one another in the carboxyl-terminal (CT) region of the protein. These C2 domains act as protein interaction domains and often mediate membrane association by means of Ca^{2+}-dependent or independent phospholipid binding.

The synaptotagmin-like proteins (SLPs) are a newly discovered family of C2 domain-containing proteins (6). In addition to their two CT C2 domains, the five mammalian SLPs share an amino-terminal SLP homology domain (SHD) that directly interacts with the vesicle-trafficking protein Rab27a (7–10). The best characterized SLP, granuphilin (also known as SLP4), also binds to the exocytosis regulatory protein Munc18 and colocalizes with insulin-containing vesicles at the cell periphery of cultured pancreatic beta cells (8, 11–14). Whereas the overexpression of wild-type and mutated versions of granuphilin can modulate the level of insulin secretion in cell culture (8, 12–14), the *in vivo* function(s) of granuphilin and the other SLPs have yet to be determined.

In this paper, we describe the characterization of an SLP gene, specifically *bitesize* (*btsz*), the only *Drosophila* SLP gene. Whereas our results do not address whether *btsz* is involved in exocytosis, they demonstrate that *btsz* is required for animal growth. Mutations that remove the function of a subset of *btsz* isoforms give rise to adults that have reduced cell size and number. Mosaic analyses indicate that *btsz* acts cell-nonautonomously, raising the possibility that it may function in growth signaling, perhaps through its putative role in exocytosis. We also show that certain *btsz* isoforms are localized to the apical plasma membrane. We define a 2.2-kb region, called the *btsz* localization region (BLR), that is necessary and sufficient to mediate apical mRNA localization. Although previous studies of localized mRNAs from a variety of organisms have shown that mRNA localization elements generally reside in untranslated regions (UTRs) of the transcript (reviewed in refs. 15 and 16), the BLR is located entirely within the *btsz* ORF. Aside from the BLR, we know of no other metazoan example of a fully functional mRNA localization sequence contained entirely within the protein-coding region of a gene.

Materials and Methods

cDNA Isolation and Characterization. All cDNAs were isolated by screening *Drosophila* embryonic (LD) and adult head (GH) cDNA libraries (17) with probes derived from clones from the CK cDNA library (18) and by 5′ RACE, which was accomplished by using the Clontech Marathon cDNA amplification kit. Potential full-length cDNAs were sequenced, analyzed with SEQUENCHER software, and searched against nucleotide and protein databases by using BLAST programs (19). The *btsz* transcription unit includes sequences that were initially thought to comprise two different genes (CG7343 and CG31306) according to the release 3.1 annotation of the *Drosophila* genome (20). We computationally searched for potential RNA secondary structures by running BLR sequences (ranging from 100 to 2,000 nt) through the MFOLD program (www.bioinfo.rpi.edu/applications/mfold).

Transformation Constructs. For constructs shown in Fig. 4, *btsz-3*, *btsz-3Δ3′UTR*, *btsz-3ΔCT*, *btsz-3ΔC2*, and *GFP-BLR* were inserted into pUAST (21); *btsz-1*, *btsz-2*, *btsz-2Δ3′UTR*, *btsz-2poly*, *btsz-2myc*, *btsz-C2*, and *GFP-CT* were inserted into pGUS (22), and their expression was driven by using *armadillo-GAL4* (S2 cells), *GMR-GAL4* (eye disc), or *heat shock* (*hs*)-GAL4 (eye discs and all other tissues). All deletion and gene-fusion constructs were derived from *btsz-1* (GenBank accession no. AY229969), *btsz-2* (accession no. AY229970), and *btsz-3* (accession no. AY229971) cDNAs, and pEGFP-C1 (Clontech; accession no. U55763). Constructs (in bold italic) are composed of the following sequences from 5′ to 3′ (polylinker sites in vectors not included): ***btsz-1***: *btsz-1* nucleotides 1–4941; ***btsz-2***: *btsz-2* nucleotides 1–8542; ***btsz-2Δ3′UTR***: *btsz-2* nucleotides 1–8081; ***btsz-2poly***: *btsz-2* nucleotides 1–7963, ATGGAATATATGCCAATGGAAATGGAATATATGCCAATGGAATAG; ***btsz-2myc***: *btsz-2* nucleotides 1–7963, ATGGAGCAGAAGCTTATCTCCGAGGAGGACCTGTAG; ***btsz-3***: *btsz-3* nucleotides 1–5530; ***btsz-3Δ3′UTR***: *btsz-3* nucleotides 1–5069; ***btsz-3ΔCT***: *btsz-3* nucleotides 1–3684, CTAG; ***btsz-3ΔC2***: AACCAA, *btsz-3* nucleotides 400-3916, TGAGTCG, *btsz-3* nucleotides 4953–5593, poly(A); ***btsz-C2***: AACCAAAATG, *btsz-3* nucleotides 3908–5593, poly(A); ***GFP-CT***: pEGFP-C1 nucleotides 591-1347, *btsz-1*

Abbreviations: CT, carboxyl-terminal; SLP, synaptotagmin-like protein; SHD, SLP homology domain; btsz, bitesize; BLR, *btsz* localization region.

Data deposition: The sequences reported in this paper have been deposited in the GenBank database (accession nos. AY229969–AY229971).

*To whom correspondence should be addressed at: Department of Molecular and Cell Biology, 515 Life Science Addition Building, University of California, Berkeley, CA 94720-3200. E-mail: serano@uclink4.berkeley.edu.

© 2003 by The National Academy of Sciences of the USA

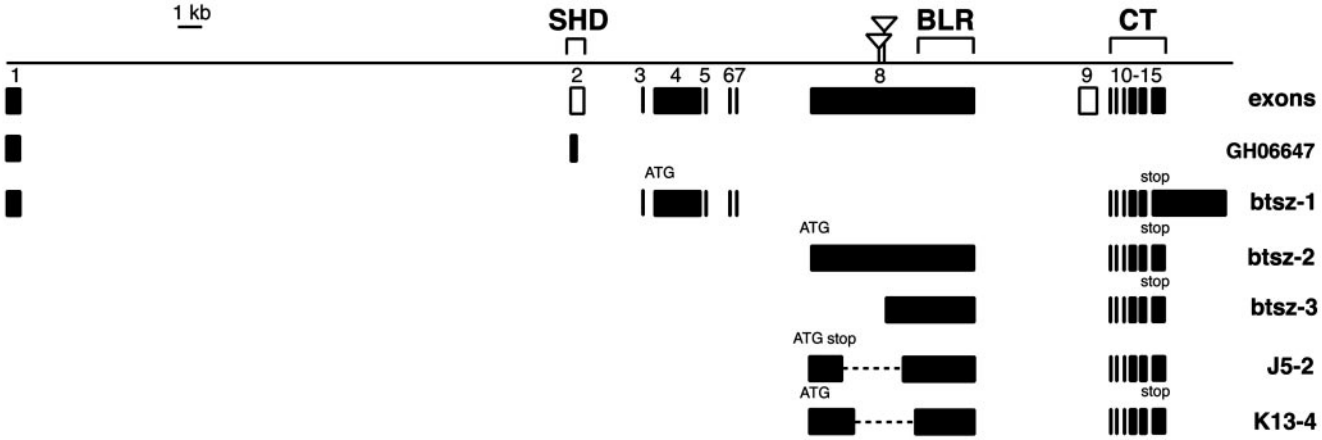

Fig. 1. Diagram of the *btsz* transcription unit. The line represents an ≈50-kb genomic region, below which are boxes (numbered 1–15) representing *btsz* exons (oriented 5′ to 3′). The solid boxes represent exons incorporated into cDNAs we isolated, and the open boxes (numbers 2 and 9) represent computationally predicted exons (release 3 of the *Drosophila* genome on www.flybase.org). Also shown are structures for a partial cDNA (GH06647), three different classes of *btsz* transcripts (*btsz-1*, *btsz-2*, and *btsz-3*), and two deletion mutants ($btsz^{J5\text{-}2}$ and $btsz^{K13\text{-}4}$) generated by mobilizing the *EP(3)3567* and *l(3)10418 P* elements (inverted triangles). The deletions are drawn in the context of the *btsz-2* transcript, which is able to rescue both mutations. The *btsz* SHD is encoded by exon 2, the *btsz* BLR is located in exon 8, and the *btsz* CT region is encoded by exons 10–15. The sequences of the diagrammed cDNAs have been deposited in the GenBank database with the following accession numbers: AY229969 (*btsz-1*), AY229970 (*btsz-2*), and AY229971 (*btsz-3*).

nucleotides 3001–5031; and ***GFP-BLR***: pEGFP-C1 nucleotides 591-1347, *btsz-2* nucleotides 4509–6695.

Genetics and Growth Experiments. The wild-type stock was w^{1118}, and all experiments were carried out in this genetic background. We generated *btsz* alleles by mobilizing the *EP(3)3567* and *l(3)10418 P* elements (23, 24), and 560 independent excision lines were screened by PCR for deletions. The $btsz^{J5\text{-}2}$ and $btsz^{K13\text{-}4}$ alleles were recombined onto the *FRT82* chromosome and mitotic clones generated as described (25). For growth experiments, flies were raised at 25°C in lightly seeded bottles. Egg-hatching experiments were carried out as previously described (26), and *btsz* mutant larvae were identified by the lack of either the *TM6b* or *TM3-armadillo-GAL4* balancers. Wings were mounted in Canada Balsam (Sigma) and photographed. Wing area was measured by using IMAGEJ software (http://rsb.info.nih.gov/ij) and cell size was determined by counting wing hairs in an 11,600-μm^2 area just posterior to the fifth cross-vein. *btsz* rescue experiments were performed by crossing transgenes into a homozygous *btsz* background along with one copy of a leaky *hs-GAL4* construct, and the resulting flies were raised at 25°C (without heat shock).

Histology and Microscopy. *In situ* hybridization and immunohistochemistry were performed as described (26). For the localization experiments in Fig. 5, ovaries carrying one copy of both *hs-GAL4* and the *btsz* construct were dissected 2–4 h after heat shock and examined by *in situ* hybridization by using probes specific for heterologous sequences in the pUAST/pGUS vectors [specifically, simian virus 40 sequences just upstream of the poly(A)-addition site]. S2 cell transfections, confocal microscopy, anti-myc and anti-polyomavirus epitope mouse antibodies, and the anti-mouse secondary antibodies, were as described (27). Fixation, embedding, and sectioning of adult eyes were performed as described (28). Standard photographs were prepared by using a Zeiss Axiophot microscope, and images were processed with PHOTOSHOP 5.5 software (Adobe Systems, Mountain View, CA).

Results and Discussion

***btsz* Gene Structure and Expression.** We first identified *btsz* in a reverse genetic screen for genes expressed during *Drosophila* development (18). The *btsz* transcription unit covers ≈50 kb and is predicted to have at least 15 exons (Fig. 1). By screening cDNA libraries, we identified three alternatively spliced forms of *btsz*, which differ in their transcription start sites and exon usage. All three isoforms share the same CT region of 423 aa. Two of these isoforms, *btsz-1* and *btsz-2*, encode proteins that are 1,099 and 2,645 aa, respectively, and do not share any sequences outside of the CT region. A third class of transcripts, *btsz-3*, is similar to *btsz-2* except that its apparent transcription start site occurs 3,013 nt farther downstream, in the middle of exon 8. It is unclear which ATG might serve as the *btsz-3* translation start site, because most of the start codons in the ORF fail to conform to the *Drosophila* start site consensus. Nevertheless, we believe that *btsz-3* is a bona fide isoform, because we isolated multiple independent clones from embryonic cDNA libraries and mapped two *P* elements to its putative transcription start site.

Whereas the amino-terminal regions of all three isoforms show no homology to any known or predicted proteins, the CT region contains two C2 domains and is most homologous (41% identities, 57% similarities) to the corresponding region of granuphilin (ref. 11; also see Fig. 6, which is published as supporting information on the PNAS web site). As with the other SLPs, neither btsz C2 domain contains the five conserved aspartate residues required for Ca^{2+}-binding. In addition, *btsz* exon 2 contains a typical SHD, including the Zn^{2+}-binding motif and conserved Rab-binding site (SGEWF), and is most homologous (44% identities, 58% similarities) to the granuphilin SHD. Although exon 2 is not present in *btsz-1*, *-2*, or *-3*, it is incorporated into the partial *btsz* cDNA GH06647 (17). Because our cDNA library screening was limited in its scope, it is likely that additional *btsz* isoforms exist.

To determine *btsz* expression, we carried out *in situ* hybridization with probes derived from different *btsz* exons. We were unable to detect any mRNA expression in embryos and imaginal discs by using probes specific to exon 2. This could be caused by low endogenous mRNA levels; or, because GH06647 was isolated from an adult head cDNA library, it is possible that exon 2 is not expressed during embryogenesis or larval development. All other tested probes revealed *btsz* expression in most cell types examined. In epithelial cells large enough to discern cell polarity, *btsz* mRNA clearly localizes to the apical plasma membrane. This localization is most obvious in follicle cells, where *btsz* transcripts accumulate along the membrane adjacent to the oocyte (Fig.

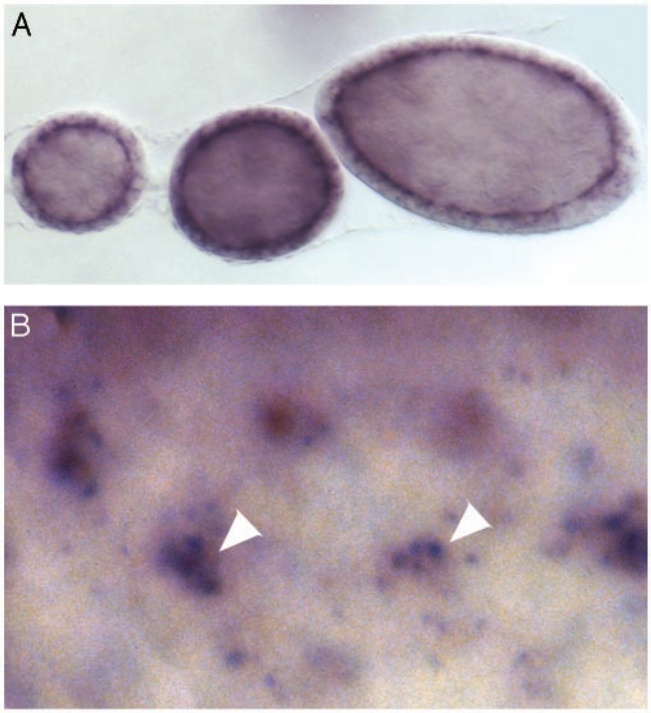

Fig. 2. *btsz* transcripts are localized. *In situ* hybridization to wild-type tissue by using probes corresponding to *btsz* exons 3–5 (*A*) or 8–15 (*B*) is shown. All probes reveal *btsz* expression in most, if not all, cell types. (*A*) During early stages of oogenesis, *btsz* mRNA is localized to the apical (oocyte-facing) surface of follicle cells. (*B*) During third-instar eye development, clusters of punctate staining are seen where the apical surfaces of different developing photoreceptors within the same ommatidium come together (white arrowheads). (Magnification: *A*, ×450; *B*, ×800.)

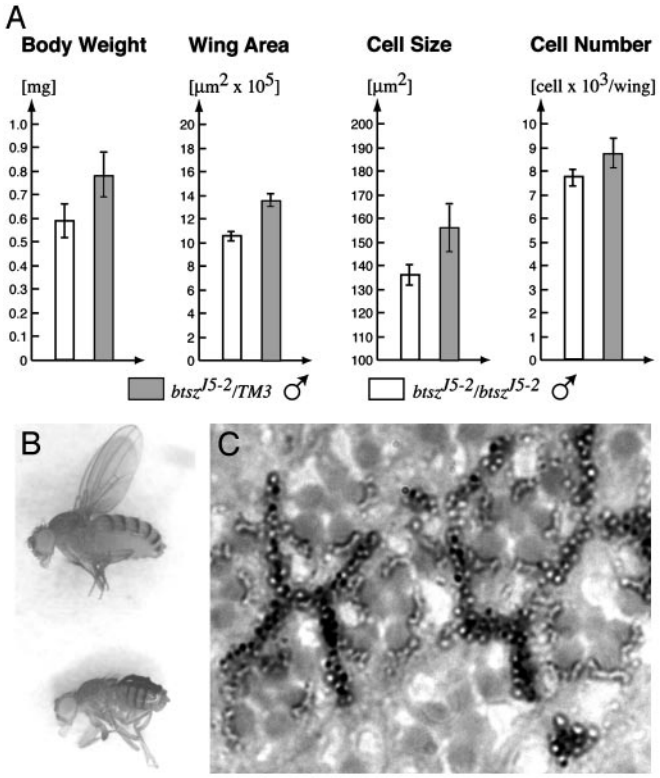

Fig. 3. *btsz* mutants exhibit growth defects. (*A*) $btsz^{J5\text{-}2}$ homozygous males (white bars) were compared with their heterozygous male siblings (gray bars) 1 day after eclosion. Values represent means with standard deviation shown as error bars. The body weight and wing area of *btsz* mutants are reduced by 23% ($n = 50$) and 21% ($n = 10$), respectively. The reduction in wing area is attributable to a 12% and 9% decrease in cell size and cell number, respectively. (*B*) Comparison of wild-type (*Upper*) and $btsz^{J5\text{-}2}$ (*Lower*) adult females. (*C*) A tangential section of a w^{1118}, *ey-FLP; FRT,* $btsz^{J5\text{-}2}$*/FRT,* $P[w^+]$, $btsz^+$ adult eye shows no obvious size difference between wild-type photoreceptor cells (marked by dark pigment) and $btsz^{J5\text{-}2}$ homozygous mutant cells (lacking pigment). (Magnification: *B*, ×10; *C*, ×1,260.)

2*A*), and in the eye imaginal disc, where clusters of staining are observed at the apical surfaces where photoreceptors within the same ommatidium contact each other (Fig. 2*B*). Probes derived from exon 8 and exons 10–15 revealed higher levels of localized *btsz* mRNA specifically in developing photoreceptors, the embryonic peripheral nervous system, and the developing oocyte (Fig. 2*B* and data not shown).

***btsz* Mutants Exhibit Growth Defects.** We identified two *P* element lines that affect *btsz*: *EP(3)3567* and *l(3)10418*. These *P* elements are inserted at positions 42 and 131 nt, respectively, upstream of the transcriptional start site of *btsz-3* (Fig. 1). Although these lines were originally reported to be homozygous-lethal, both *P* element insertions were found to be viable after removal of second-site mutations. We generated *btsz* loss-of-function mutations by *P* element imprecise excision and isolated two lines with deletions on the order of 2.5 kb. $btsz^{J5\text{-}2}$ was derived from *EP(3)3567* and contains a frameshift mutation that results in a truncated btsz-2 protein of 393 aa. $btsz^{K13\text{-}4}$ was derived from *l(3)10418* and removes ≈991 aa from the btsz-2 protein, but does not alter the reading frame. Although $btsz^{J5\text{-}2}$ is a slightly stronger allele than $btsz^{K13\text{-}4}$, both mutants give rise to a similar set of phenotypes (both as homozygotes and as transheterozygotes) and both are partially rescued by ubiquitous expression of *btsz-2* (Fig. 4). It is not surprising that this rescue is only partial, because there are multiple *btsz* isoforms that use exon 8 (Fig. 1). Because of the lack of deficiencies in the *btsz* region, we were unable to test whether these mutations are likely to remove the complete activity of isoforms *btsz-2* and *btsz-3*. It should be noted that expression of *btsz-1*, which does not incorporate exon 8, is not able to rescue the *btsz* alleles we have isolated.

About 95% ($n = 271$) of the progeny from a $btsz^{J5\text{-}2/+}$ cross hatch as larvae, indicating that *btsz* is not embryonic-lethal. This lack of embryonic lethality may be the result of a maternal contribution, as certain *btsz* isoforms are localized to the oocyte. During larval stages, *btsz* mutants develop more slowly than their heterozygous siblings, generally taking two extra days to reach the wandering third-instar stage. Only 70% ($n = 654$) of $btsz^{J5\text{-}2}$ mutant larvae survive to the third-instar stage, but they appear normal with regards to feeding and movement. Adult *btsz* mutants eclose 2–3 days after their heterozygous siblings and are smaller than wild type: $btsz^{J5\text{-}2}$ homozygous flies are 77% the weight and have 79% the wing area of their heterozygous siblings (Fig. 3 *A* and *B*). Examination of wing hair density reveals that the *btsz* growth phenotype is attributable to a reduction in both cell size and number. In addition, *btsz* mutants display other phenotypes common among genes involved in growth, including reduced body pigmentation; shorter, thinner bristles; slightly rough eyes; occasionally crumpled wings; and fewer eggs laid by females (data not shown; see refs. 29–32). Despite these phenotypes, *btsz* adults are properly proportioned and show no obvious defects in coordination, feeding, or mating behavior.

To determine whether *btsz* functions cell-autonomously, we used the FLP/FRT system to produce *btsz* mutant cells in an otherwise wild-type background (25). We generated *btsz* clones randomly throughout the body by using *heat shock-FLP recombinase* (*hs-FLP*) or specifically in the eye imaginal disc by using

eyeless-FLP recombinase (*ey-FLP*). Sections of eyes containing *btsz* clones revealed no obvious differences in size between wild-type and *btsz* ommatidia, nor were there any size differences between wild-type and mutant photoreceptor cells within the same ommatidium (Fig. 3*C*). It is difficult to draw strong conclusions on this result alone, because experiments in wing discs indicate that *btsz* mutant cells are only 12% smaller than wild type (Fig. 3*A*), a difference that might be difficult to detect at the individual cell level. However, *btsz* clones generated by *hs-FLP* were comparable in size to their wild-type twin spots, indicating that *btsz* cells are able to grow and proliferate normally (data not shown). This was also the case when clones were generated in a *Minute* background. Although *hs-FLP*-induced *btsz* clones costituted from 0% to 15% of the adult eye in a wild-type background, these clones ranged from 70% to 85% in a *M(3)95A* background; wild-type controls yielded similar clone sizes in both backgrounds. Together, these results suggest that *btsz* acts cell-nonautonomously with respect to cell growth and proliferation. It should be noted that the only *btsz* mosaic animals to display growth defects were those in which *btsz* clones were generated in a *M(3)95A* background. We have not been able to determine whether this phenotype is caused by removing *btsz* function by a specific subset of cells or from an overall reduction in the number of cells having *btsz* activity throughout the animal.

The fact that *btsz* appears to have a nonautonomous growth phenotype and shares homology to granuphilin, a protein implicated in vertebrate insulin secretion, raises the possibility that *btsz* growth defects are the result of reduced insulin signaling in flies. Although this model is intriguing, we have been unable to detect any genetic interactions between *btsz* and the *Drosophila* insulin receptor (31, 32). Furthermore, our genetic and immunohistochemical data demonstrate that functional ILP2 (one of the seven *Drosophila* insulin-like proteins; ref. 33) is produced in *btsz* mutants (data not shown). Because the *btsz* growth phenotype can be partially rescued by *btsz-2*, which does not contain the SHD, it is possible that btsz provides a role other than vesicle trafficking or exocytosis in the regulation of growth.

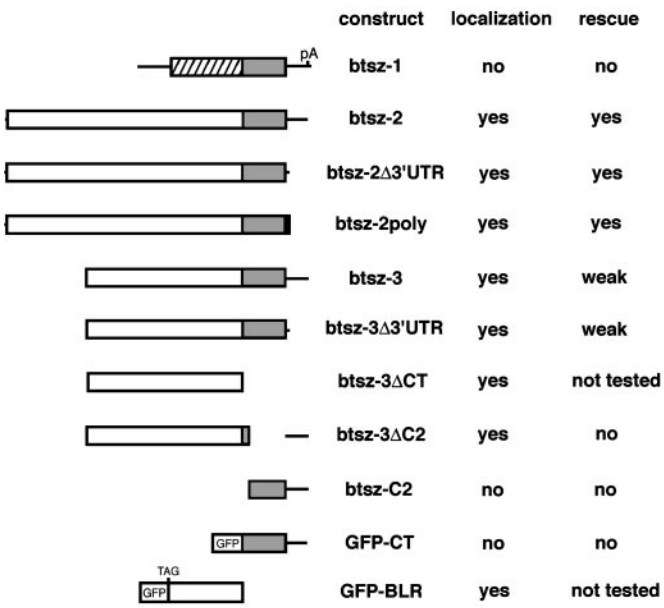

Fig. 4. Mapping of sequences sufficient for *btsz* rescue and apical mRNA localization. Schematic diagrams of 11 transgenic constructs derived from *btsz* cDNAs (Fig. 1) are shown. The differently shaded rectangles correspond to either *btsz-1*-specific exons (hatched), two copies of the polyoma epitope tag (black), sequences from exon 8 (white), the CT region (gray), or the GFP-coding region (white with ''GFP''; precise sequences described in text). Lines represent UTRs. The *btsz-2myc* construct is identical to *btsz-2poly*, except that the myc epitope replaces two copies of the polyoma epitope. Each construct also contains identical simian virus 40 3′-UTR sequences provided by the pUAST or pGUS vectors (not shown). All lines were crossed to *hs-GAL4* to determine whether they can rescue the *btsz* mutant phenotype (rescue) or produce apically localized mRNA in follicle cells (localization). Constructs with a ''yes'' in the rescue column fully restore the *btsz* viability and bristle, wing, and pigmentation phenotypes and partially rescue the *btsz* growth defects to yield a phenotype intermediate between *btsz* mutants and wild type.

***btsz* Localization.** To gain further insight into *btsz* function, we examined the subcellular localization of btsz-2 proteins carrying the polyoma or myc epitope at their carboxyl termini. Both *btsz-2poly* and *btsz-2myc* produced functional protein as assayed by their ability to rescue *btsz* mutants (Fig. 4). When these constructs were transfected into S2 cells, tagged btsz-2 protein localized along the plasma membrane (Fig. 5*A*). A similar localization pattern was seen when the *btsz* CT region was fused to GFP, indicating that plasma membrane association of btsz-2 protein is mediated by this region (data not shown). Next, we determined btsz-2 protein localization in polarized cells. We used *hs-GAL4* to drive *btsz-2poly* and *btsz-2myc* expression in follicle cells, where endogenous *btsz* transcripts localize apically. Around 1.5–2 h after heat shock, we detected btsz-2 protein along the apical plasma membrane of follicle cells (Fig. 5*B*). We did not observe any changes in the localization pattern of tagged btsz-2 proteins over time (up to 7.5 h after heat shock) and we were unable to detect any protein localization to intracellular vesicles.

When we examined *btsz-2poly* and *btsz-2myc* mRNA expression in follicle cells, we found that transcripts localized to the follicle cell apical plasma membrane in a manner indistinguishable from an untagged *btsz-2* construct (Fig. 5*C* and data not shown). Control constructs that express *GFP*, *lacZ*, or the transcription factor *tramtrack* produced mRNA that is not localized (data not shown), demonstrating that sequences within the vectors did not confer localization. Aside from the epitope tags, *btsz-2poly* and *btsz-2myc* differ from *btsz-2* only in their lack of *btsz* 3′-UTR sequences (Fig. 4). Thus, unlike the vast majority of localized mRNAs, *btsz* does not require 3′-UTR sequences for localization.

To further delimit the *btsz* mRNA localization sequences, we performed similar experiments with transgenes derived from the *btsz-1* and *btsz-3* transcripts. We found that *btsz-1* transcripts were not localized (Fig. 5*D*), indicating that *btsz* mRNA localization is not mediated by the sequences shared by all three *btsz* isoforms (namely the CT region and the 3′ UTR). In contrast, *btsz-3* produced apically localized mRNA (Fig. 5*E*). These results suggest that all of the sequences required for *btsz* mRNA localization reside in exon 8, which is incorporated into *btsz-2* and *btsz-3* but not *btsz-1*. To test this possibility, we constructed *btsz-3ΔCT*, which corresponds to the 3.7-kb region of exon 8 shared by *btsz-2* and *btsz-3* (Fig. 4). As seen in Fig. 5*F*, *btsz-3ΔCT* transcripts were localized apically, demonstrating that the sequences necessary and sufficient for *btsz* mRNA localization are contained within the ORF included in exon 8. Because $btsz^{J5\text{-}2}$ and $btsz^{K13\text{-}4}$ mutants also produced apically localized transcripts (Fig. 5 *G* and *H*) despite having deletions that remove large portions of exon 8, the sequences important for *btsz* localization were narrowed down to a 2.2-kb fragment that we named the BLR. To determine whether the BLR is sufficient for apical mRNA localization, we placed it out of frame and downstream of the stop codon of *GFP* to make *GFP-BLR*. As a control, we used *GFP-CT*, which consists of *GFP* fused to the *btsz* CT region and the 3′ UTR (Fig. 4). *GFP-BLR* transcripts are apically localized in follicle cells and in cells of the eye and wing imaginal discs (Fig. 5 *I*, *K*, and *M*), unlike *GFP-CT* transcripts, which remain unlocalized (Fig. 5 *J*, *L*, and *N*). This result demonstrates that the BLR is sufficient for apical mRNA localization, even in a heterologous context, and rules out the possibility that apical localization is mediated by the polypeptide encoded by the BLR.

The BLR is a metazoan example of a fully functional mRNA

DEVELOPMENTAL BIOLOGY

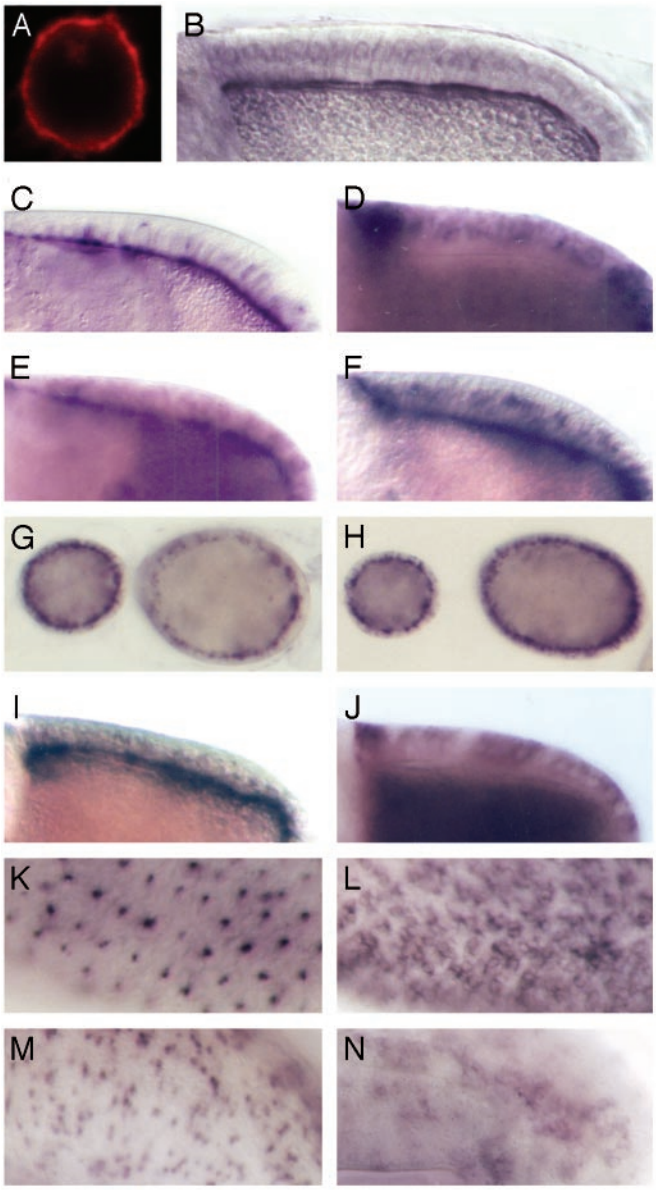

Fig. 5. *btsz* apical localization is mediated by the BLR. Various *btsz* transgenes were expressed by using the GAL4/UAS system (for schematic diagrams of *btsz* constructs, see Fig. 4). (*A* and *B*) btsz-2 protein fused to a polyoma epitope tag (btsz-2poly) localizes to the plasma membrane of S2 tissue culture cells (*A*) and the apical surface of follicle cells (*B*). (*C–F*) Follicle cells expressing *btsz-2* (*C*), *btsz-1* (*D*), *btsz-3* (*E*), and *btsz3ΔCT* (*F*). Whereas *btsz-2poly*, *btsz-2*, *btsz-3*, and *btsz3ΔCT* transcripts are localized to the apical (oocyte-facing) surface of follicle cells, *btsz-1* is not. (*G* and *H*) Apical mRNA localization of endogenous *btsz* transcripts in $btsz^{J5\text{-}2}$ (*G*) and $btsz^{K13\text{-}4}$ (*H*) follicle cells. (*I–N*) Expression of *GFP-BLR* (*I*, *K*, and *M*) and *GFP-CT* (*J*, *L*, and *N*) transcripts in follicle cells (*I* and *J*) and third-instar eye (*K* and *L*) and wing (*M* and *N*) imaginal discs. *GFP-BLR* transcripts localize to the apical surface, whereas *GFP-CT* transcripts are uniformly distributed within the cells that express them. (Magnification: *A*, ×1,500; *B–N*, ×300.)

localization sequence contained entirely within the protein-coding region of a gene. The only other known example of a localized transcript containing protein-coding sequences sufficient to reproduce the wild-type localization pattern is the yeast *ASH1* gene. The localization of *ASH1* mRNA to the yeast bud tip can be mediated by any one of three cis-acting elements; two of these elements are located entirely within the ORF, and the third spans the ORF and the 3′ UTR (34, 35). Other localized mRNAs, namely rat *vasopressin precursor* and *Drosophila gurken* and *yem-alpha*, appear to require a contribution from protein-coding sequences for localization, but such sequences have not been shown to be sufficient to reconstitute the wild-type localization pattern (36–39). One might expect the presence of mRNA localization elements within the *btsz* ORF to interfere with its translation. For example, localization factors bound to the BLR might prevent ribosomes from reading through the coding region; or, alternatively, translation through the BLR might uncouple the transcript from localization factors, allowing the mRNA to diffuse freely after its initial localization. Interestingly, *ASH1* mRNA translation is a requirement for complete localization to the daughter cell cortex, suggesting that ribosomes may anchor transcripts once they reach their final destination (35). A similar form of translation-dependent anchoring might play a role in *btsz* localization.

Although a number of proteins implicated in exocytosis are localized to specific regions along the apical–basal axis (40–43), at this time it is not clear whether *btsz* apical localization is required for its gene function. The BLR does contain a number of sequence stretches that show extensive nucleotide-level homology with the *Anopheles gambiae* (mosquito) *btsz* gene (ref. 44 and unpublished data). In fact, one 59-nt region of the BLR is 92% conserved between flies and mosquito. (Only 77% nucleotide identity would be expected if both sequences encoded identical peptides.) Such conserved sequences may represent functionally conserved mRNA localization elements. Previous studies on other localized mRNAs have shown that mRNA localization elements often form stem-loop structures that are important for their localization (34, 35, 45–47). On examination of the BLR by using computer algorithms designed to identify RNA secondary structures, we found one predicted stable stem-loop structure (*btsz-2* nucleotides 5311–5405), although its importance is not clear, because the secondary structure is not conserved in *Anopheles*. Once the primary sequence and/or secondary structures required for *btsz* apical mRNA localization are determined, it should be possible to create mutations that disrupt *btsz* localization without affecting btsz protein function. Such experiments may provide additional insight into what functional differences exist between *btsz* isoforms and what role(s) each isoform plays in animal growth and, possibly, exocytosis.

We thank Martha Evans-Holm, Elaine Kwan, Todd Laverty, Susan Mullaney, John Pendelton, and Garson Tsang for technical help; Adina Bailey, Mike Brodsky, Ernst Hafen, Eric Rufilson, Kathy Sullivan, and Amy Hong Tang for fly stocks and reagents; and Bob Cohen, Audrey Huang, Eric Lai, Andrea Page-McCaw, Kathy Sullivan, and Amy Hong Tang for providing helpful comments. J.S. was supported by a Leukemia and Lymphoma Society Special Fellow Award. G.M.R. is an investigator of the Howard Hughes Medical Institute.

1. Südhof, T. C. & Rizo, J. (1996) *Neuron* **17,** 379–388.
2. Shirataki, H., Kaibuchi, K., Sakoda, T., Kishida, S., Yamaguchi, T., Wada, K., Miyazaki, M. & Takai, Y. (1993) *Mol. Cell. Biol.* **13,** 2061–2068.
3. Wang, Y., Sugita, S. & Südhof, T. C. (2000) *J. Biol. Chem.* **275,** 20033–20044.
4. Duncan, R. R., Shipston, M. J. & Chow, R. H. (2000) *Biochimie* **82,** 421–426.
5. Brose, N., Rosenmund, C. & Rettig, J. (2000) *Curr. Opin. Neurobiol.* **10,** 303–311.
6. Fukuda, M. & Mikoshiba, K. (2001) *Biochem. Biophys. Res. Commun.* **281,** 1226–1233.
7. Fukuda, M., Saegusa, C. & Mikoshiba, K. (2001) *Biochem. Biophys. Res. Commun.* **283,** 513–519.
8. Yi, Z., Yokota, H., Torii, S., Aoki, T., Hosaka, M., Zhao, S., Takata, K., Takeuchi, T. & Izumi, T. (2002) *Mol. Cell. Biol.* **22,** 1858–1867.
9. Kuroda, T. S., Fukuda, M., Ariga, H. & Mikoshiba, K. (2002) *J. Biol. Chem.* **277,** 9212–9218.

10. Kuroda, T. S., Fukuda, M., Ariga, H. & Mikoshiba, K. (2002) *Biochem. Biophys. Res. Commun.* **293,** 899–906.
11. Wang, J., Takeuchi, T., Yokota, H. & Izumi, T. (1999) *J. Biol. Chem.* **274,** 28542–28548.
12. Coppola, T., Frantz, C., Perret-Menoud, V., Gattesco, S., Hirling, H. & Regazzi, R. (2002) *Mol. Biol. Cell* **13,** 1906–1915.
13. Torii, S., Zhao, S., Yi, Z., Takeuchi, T. & Izumi, T. (2002) *Mol. Cell. Biol.* **22,** 5518–5526.
14. Fakuda, M. (2003) *J. Biol. Chem.* **278,** 5390–15396.
15. Palacios, I. M. & St. Johnston, D. (2001) *Annu. Rev. Cell Dev. Biol.* **17,** 569–614.
16. Kloc, M., Zearfoss, N. & Etkin, L. D. (2002) *Cell* **108,** 533–544.
17. Rubin, G. M., Hong, L., Brokstein, P., Evans-Holm, M., Frise, E., Stapleton, M. & Harvey, D. A. (2000) *Science* **287,** 2222–2224.
18. Kopczynski, C. C., Noordermeer, J. N., Serano, T. L., Chen, W. Y., Pendleton, J. D., Lewis, S., Goodman, C. S. & Rubin, G. M. (1998) *Proc. Natl. Acad. Sci. USA* **95,** 9973–9978.
19. Altschul, S. F., Gish, W., Miller, W., Myers, E. W. & Lipman, D. J. (1990) *J. Mol. Biol.* **215,** 403–410.
20. Misra, S., Crosby, M. A., Mungall, C. J., Matthews, B. B., Campbell, K. S., Hradecky, P., Huang, Y., Kaminker, J. S., Millburn, G. H., Prochnik, S. E., *et al*. (2002) *Genome Biol.* **3,** 83.1–83.22.
21. Brand, A. H. & Perrimon, N. (1993) *Development (Cambridge, U.K.)* **118,** 401–415.
22. Brodsky, M. H., Sekelsky, J. J., Tsang, G., Hawley, R. S. & Rubin, G. M. (2000) *Genes Dev.* **14,** 666–678.
23. Rørth, P. (1996) *Proc. Natl. Acad. Sci. USA* **93,** 12418–12422.
24. Spradling, A. C., Stern, D., Beaton, A., Rhem, E. J., Laverty, T., Mozden, N., Misra, S. & Rubin, G. M. (1999) *Genetics* **153,** 135–177.
25. Xu, T. & Rubin, G. M. (1993) *Development (Cambridge, U.K.)* **117,** 1223–1237.
26. Serano, T. L. & Cohen, R. S. (1995) *Development (Cambridge, U.K.)* **121,** 3013–3021.
27. Tang, A. H., Neufeld, T. P., Kwan, E. & Rubin, G. M. (1997) *Cell* **90,** 459–467.
28. Wolff, T. & Ready, D. F. (1991) *Development (Cambridge, U.K.)* **113,** 825–839.
29. Lambertsson, A. (1998) *Adv. Genet.* **38,** 69–134.
30. Johnston, L. A., Prober, D. A., Edgar, B. A., Eisenman, R. N. & Gallant, P. (1999) *Cell* **98,** 779–790.
31. Fernandez, R., Tabarini, D., Azpiazu, N., Frasch, M. & Schlessinger, J. (1995) *EMBO J.* **14,** 3373–3384.
32. Chen, C., Jack, J. & Garofalo, R. S. (1996) *Endocrinology* **137,** 846–856.
33. Brogiolo, W., Stocker, H., Ikeya, T., Rintelen, F., Fernandez, R. & Hafen, E. (2001) *Curr. Biol.* **11,** 213–221.
34. Chartrand, P., Meng, X.-H., Singer, R. H. & Long, R. M. (1999) *Curr. Biol.* **9,** 333–336.
35. Gonzalez, I., Buonomo, S. B. C., Nasmyth, K. & von Ahsen, U. (1999) *Curr. Biol.* **9,** 337–340.
36. Prakash, N., Fehr, S., Mohr, E. & Richter, D. (1997) *Eur. J. Neurosci.* 523–532.
37. Saunders, C. & Cohen, R. S. (1999) *Mol. Cell* **3,** 43–54.
38. Thio, G. L., Ray, R. P., Barcelo, G. & Schüpbach, T. (2000) *Dev. Biol.* **221,** 435–446.
39. Capri, M., Santoni, M.-J., Thomas-Delaage, M. & Ait-Ahmed, O. (1997) *Mech. Dev.* **68,** 91–100.
40. Low, S. H., Chapin, S. J., Weimbs, T, Kömüves, L. G., Bennett, M. K. & Mostov, K. E. (1996) *Mol. Biol. Cell* **7,** 2007–2018.
41. Riento, K., Galli, T., Jansson, S., Ehnholm, C., Lehtonen, E. & Olkkonen, V. M. (1998) *J. Cell Sci.* **111,** 2681–2688.
42. Quiñones, B., Riento, K., Olkkonen, V. M., Hardy, S. & Bennett, M. K. (1999) *J. Cell Sci.* **112,** 4291–4304.
43. Müsch, A., Cohen, D., Yeaman, C., Nelson, W. J., Rodriguez-Boulan, E. & Brennwald, P. J. (2002) *Mol. Biol. Cell* **13,** 158–168.
44. Holt, R. A., Subramanian, G. M., Halpern, A., Sutton, G. G., Charlab, R., Nusskern, D. R., Wincker, P., Clark, A. G., Ribeiro, J. M. C., Wides, R., *et al*. (2002) *Science* **298,** 129–149.
45. Serano, T. L. & Cohen, R. S. (1995) *Development (Cambridge, U.K.)* **121,** 3809–3818.
46. Ferrandon, D., Koch, I., Westhof, E. & Nüsslein-Volhard, C. (1997) *EMBO J.* **16,** 1751–1758.
47. MacDonald, P. M. & Kerr, K. (1998) *Mol. Cell. Biol.* **18,** 3788–3795.